

## Elastic circles in 2-spheres

This article has been downloaded from IOPscience. Please scroll down to see the full text article.

2006 J. Phys. A: Math. Gen. 39 2307

(<http://iopscience.iop.org/0305-4470/39/10/005>)

View [the table of contents for this issue](#), or go to the [journal homepage](#) for more

Download details:

IP Address: 171.66.16.101

The article was downloaded on 03/06/2010 at 04:13

Please note that [terms and conditions apply](#).

## Elastic circles in 2-spheres

J Arroyo, O J Garay and J Mencía

Departamento de Matemáticas, Facultad de Ciencia y Tecnología, Universidad del País Vasco/Euskal Herriko Unibertsitatea, Apto 644, 48080 Bilbao, Spain

E-mail: [mparolj@lg.ehu.es](mailto:mparolj@lg.ehu.es), [oscarj.garay@ehu.es](mailto:oscarj.garay@ehu.es) and [mtpmegoj@lg.ehu.es](mailto:mtpmegoj@lg.ehu.es)

Received 10 June 2005, in final form 28 December 2005

Published 22 February 2006

Online at [stacks.iop.org/JPhysA/39/2307](http://stacks.iop.org/JPhysA/39/2307)

### Abstract

By solving the Euler–Lagrange equations, we determine the elastic curves in the two-dimensional sphere which are circular at rest. We characterize the family of closed critical curves by a rational condition and the existence of closed elastic curves for the different possible values of their curvature at rest is proved. In the final part of the paper, we utilize a numerical approach to get a better understanding of the space of closed critical curves. In this manner we analyse their shape, uniqueness and minimizing properties.

PACS numbers: 02.30.Xx, 02.40.Hw, 02.40.Yy, 45.20.Jj

### 1. Introduction

Let us consider a thin stiff rod in Euclidean space which is in the shape of a straight line when no forces act on it. Let us bend the rod and assume that it has a circular cross-section everywhere. Then the bent rod can be described as a regular curve  $\gamma : I \rightarrow \mathbb{R}^3$  whose elastic energy is given by  $\int_{\gamma} \kappa^2$ , where  $\kappa$  is the curvature of  $\gamma$ . This can be generalized to the case of a stiff rod with a circular cross-section, having an arbitrary shape of curvature  $\kappa_0$  in its undeformed state. The bending energy in this case is given by

$$\mathcal{F}(\gamma) = \int_{\gamma} (\kappa - \kappa_0)^2. \quad (1)$$

Equilibrium positions of the stiff bent rod can be studied by computing the critical points of (1) under the boundary conditions determined by the concrete problem we wish to analyse [6]. If  $\gamma$  is a plane curve and  $\kappa_0 = 0$  (respectively,  $\kappa_0 = \text{constant} \neq 0$ ) the above problem corresponds to the classical model for elastic curves which are straight lines at rest (respectively, a circle at rest) proposed by D Bernoulli around 1740. This geometric approach can be used to model stiff polymers, vortices in fluids, superconductors, membranes and mechanical properties of DNA molecules. (For more details see [5] and the references therein.)

Actually, denoting the geodesic curvature by  $\kappa$ , the variational problem induced by (1) can be considered in any Riemannian manifold  $\mathbb{M}^n$ . Most interesting cases occur when  $\mathbb{M}^n$

is a space of constant curvature. Also, since closed critical points are of special geometric significance, we shall focus our attention on closed critical curves. Under these assumptions,  $n$  must be at most three and elastic curves have been used to produce examples of axis-symmetric vesicles and Hopf vesicles under the Canham–Helfrich model [2, 5].

From now on, we restrict ourselves to the case in which  $\kappa_0 = \text{constant} = -\lambda$  and  $n = 2$ . At this point, it is also interesting to consider critical points of the bending energy for variations with constant length. The energy functional to be minimized in this case is  $\mathcal{F}_\mu^\lambda(\gamma) = \int_\gamma (\kappa + \lambda)^2 + \mu$ .

Assume first that  $\mathbb{M}^n = \mathbb{R}^2$ . If  $\lambda = 0$ , critical points of  $\mathcal{F}_\mu^\lambda$  are the classical elastica of Bernoulli. Their possible shapes were discovered by L Euler. There are no closed plane free elastica ( $\mu = 0$ ), but if one admits a constraint on the length ( $\mu \neq 0$ ), then in addition to non-closed examples also circles and Bernoulli eight-curves appear. Classical plane elastica have also been classified under different boundary conditions by A Linner [8]. Clearly, since the total curvature is constant on a regular homotopy class of plane curves, no new examples of plane elastica appear if one considers  $\lambda \neq 0$ .

Thus, the next natural step is the analysis of closed critical points of

$$\mathcal{F}^\lambda(\gamma) = \int_\gamma (\kappa + \lambda)^2 \quad (2)$$

in the 2-sphere. In this case, critical points of (2) correspond to elastic curves in  $\mathbb{S}^2(1)$  which are circles of curvature  $-\lambda$  at rest and with no penalty on the length. We point out that this functional is affected by the orientation of the curve: if  $\gamma(s)$  is a critical point of  $\mathcal{F}^\lambda$ , then  $\gamma(-s)$  is a critical point of  $\mathcal{F}^{-\lambda}$ . So we may assume  $\lambda \geq 0$  and critical points of (2) will be called  $\lambda$ -elastic curves for simplicity. Hence, our task will be to study closed  $\lambda$ -elastic curves in  $\mathbb{S}^2(1)$ . Closed  $\lambda$ -elastic curves in the hyperbolic plane  $\mathbb{H}^2(-1)$  will be analysed in a forthcoming paper [3].

A careful analysis of this problem would require to complete the following process: (i) computation and integration of the Euler–Lagrange (EL) equations; (ii) finding the periodic solutions of the EL equations; (iii) establishing closedness conditions for those curves associated with them; (iv) classification of the closed critical curves; (v) stability and determination of the local minima.

This program has been completed by J Langer and D Singer for classical elastica ( $\lambda = 0$ ) in [7]. In section 2, we show how one can use their techniques in order to fulfil steps (i) to (iii): from the first variation formula one can obtain the EL equation as a second-order ODE expressed in terms of the curvature  $\kappa$  of the critical curve  $\gamma$ . Moreover, restriction to the space of closed curves results in that the boundary term of the first variation formula vanishes. Once periodic solutions of the EL equation are found, we establish a closedness criterion in terms of the curvature of the critical curve (see proposition 1). Then, we use it to prove the existence of an infinite family of closed critical curves for any  $\lambda \neq 0$ . In [2] we made this analysis for the particular case  $\lambda > 8$  and  $d \in (\delta_1, \delta_2)$  (see section 2 for the meaning of these parameters) with the purpose of constructing new examples of Hopf vesicles in  $\mathbb{S}^3(1)$ .

We note, however, that questions (iv) and (v) are more subtle for  $\lambda \neq 0$  and require much more elaborate constructions. For a given  $\lambda$ , the space of periodic solutions to the EL equations depends on a real parameter  $d > 0$ . A critical curve  $\gamma$  will be closed if its angular variation in one period of its curvature is a rational multiple of  $\pi$ . This gives a condition to be satisfied by  $d$  which might be used to classify the closed critical points. However, for most values of  $\lambda$ , although we can prove the existence of values of  $d$  satisfying the closedness condition, we cannot express it explicitly in terms of  $d$ . But even when this is possible, the

explicit expression is so complicated that it is hard to derive good information for classification purposes.

On the other hand, in order to determine the critical points with minimum energy, one may want to obtain the second variation formula of  $\mathcal{F}^\lambda(\gamma)$ . We have computed it in [1], but the expression for the curvature function makes it very difficult to handle except for the simplest cases: stability of the constant curvature critical curves was determined in [2] for  $\lambda > 8$ . Apart from the case  $\lambda = 0$ , where geodesics are the only stable closed critical points [7], it is not known whether or not there are stable closed critical curves with non-constant curvature.

Hence, one might try to get some numerical insight concerning steps (iv) and (v), and then infer some properties of the space of closed solutions. We make this analysis numerically in section 3. By using a coordinate system especially adapted to the problem, where the coordinates of the closed critical points can be obtained by quadratures and the closedness conditions can be clearly stated, we design an algorithm which is well suited to carry over this numerical investigation and that can be combined with available software in order to obtain graphical information and derive plausible hypothesis. Some of them can be formally proved as explained in section 3, while others can be used as strong support for open working lines. Finally, some technical results are banished to the appendices in section 4. Computer programming and tedious numerical algorithms are not included.

## 2. $\lambda$ -elastic curves in $\mathbb{S}^2(1)$

Let  $\gamma(t)$  be a regular curve in  $\mathbb{S}^2(1)$ , that is  $\gamma : [0, 1] \rightarrow \mathbb{S}^2(1)$  is a  $C^\infty$  immersion in the two-dimensional standard unit sphere. We let  $s$  denote the arclength parameter and we use  $\gamma(s), \kappa(s)$  for the corresponding reparametrization and for the curvature function of  $\gamma(t)$  respectively. Given a real number  $\lambda \geq 0$ , we consider the variational problem of minimizing the functional

$$\mathcal{F}^\lambda(\gamma) = \int_\gamma (\kappa + \lambda)^2 ds, \quad (3)$$

amongst the set of closed immersed curves in  $\mathbb{S}^2(1)$ . The first variation formula of  $\mathcal{F}^\lambda$  can be computed by using standard arguments. For completeness, we give a short derivation of this formula in appendix A. As we explained in the introduction, we shall focus on  $\mathcal{F}^\lambda$  acting on closed curves, although there are other natural choices of boundary data for which the boundary term in the first variation formula drops out. From the first variation formula (see (A.4) and (A.5)) we obtain that a critical point of  $\mathcal{F}^\lambda$  will satisfy the following Euler–Lagrange equation

$$2\kappa_{ss} + \kappa^3 + (2 - \lambda^2)\kappa + 2\lambda = 0, \quad (4)$$

where the subscript  $s$  denotes differentiation with respect to the arclength. Circles of curvature  $\eta_0 = -\lambda$  are trivial solutions of (4) and absolute minima of (3). If  $\lambda^2 < 8$ , there are no other critical circles. If  $\lambda^2 > 8$ , circles of curvature  $\eta_1 = \frac{\lambda + \sqrt{\lambda^2 - 8}}{2}$  and  $\eta_2 = \frac{\lambda - \sqrt{\lambda^2 - 8}}{2}$  are also critical points. Assume that  $\kappa(s)$  is not constant. Multiplying (4) by  $\kappa_s(s)$  we obtain a first integral

$$4\kappa_s^2 = d - (\kappa + \lambda)^2((\kappa - \lambda)^2 + 4), \quad (5)$$

where  $d > 0$  is a real constant. Denote by  $Q_d(x) = d - (x + \lambda)^2((x - \lambda)^2 + 4)$ ,  $d > 0$ . By using the method of phase portraits for instance, one can see that non-constant solutions of (5) are periodic functions. Actually, it can be proved that they are given by elliptic functions. For our purposes however, we will need to solve (5) explicitly. When solving  $\int \frac{d\kappa}{Q_d(\kappa)^{\frac{1}{2}}} = \pm \frac{1}{2} \int ds$ , one can discuss the solutions of (5) in terms of the roots of the polynomial  $Q_d(x)$ , being its

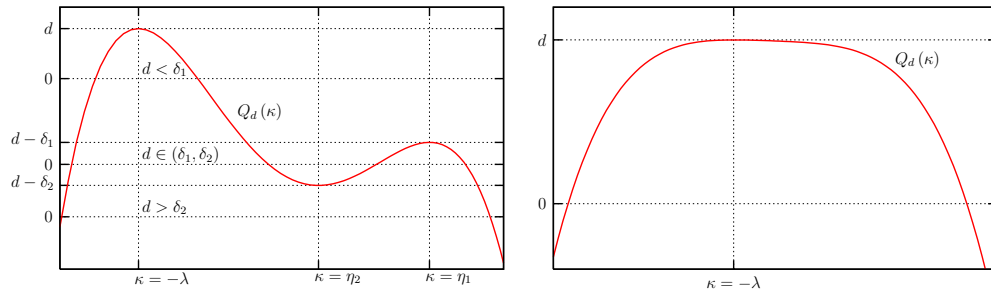


Figure 1. Pictures of  $Q_d$  corresponding to the four-root and two-root cases respectively.

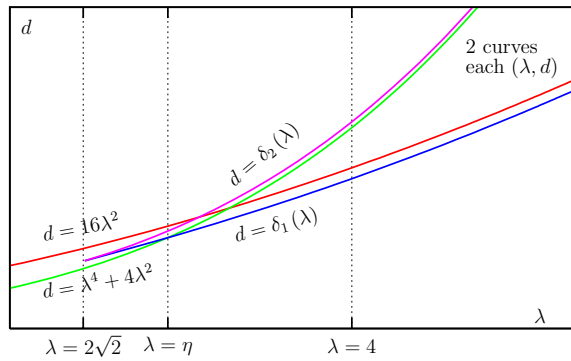


Figure 2. Evolution of the different parameters depending on  $\lambda$ .

Table 1. For  $\lambda = 2\sqrt{2}$  first column also applies as long as  $d \neq 108$ .

Roots of $Q_d$	$\lambda < 2\sqrt{2}$	$2\sqrt{2} < \lambda < \eta$	$\lambda > \eta$
$\alpha_1 < \alpha_2 < 0$	$d < \xi$	$d < \xi$	$d < \delta_1 < \xi$
$\alpha_1 < \alpha_2 = 0$	$d = \xi$	$d = \xi$	NO
$\alpha_1 < \alpha_2 < 0 < \alpha_3 < \alpha_4$	NO	NO	$\delta_1 < d < \xi$
$\alpha_1 < \alpha_2 = 0 < \alpha_3 < \alpha_4$	NO	NO	$d = \xi$
$\alpha_1 < 0 < \alpha_2 < \alpha_3 < \alpha_4$	NO	$\delta_1 < d < \delta_2$	$\xi < d < \delta_2$
$\alpha_1 < 0 < \alpha_2$	$d > \xi$	$\xi < d < \delta_1$ or $d > \delta_2$	$d > \delta_2$

multiple roots those which affect the integrability. If  $Q_d(x)$  has no multiple roots, then it admits either 2 or 4 simple roots (see figure 1), depending on the values of the parameters  $\lambda$  and  $d$  (see table 1 and figure 2), where we have set  $Q_0(x) = -(x + \lambda)^2((x - \lambda)^2 + 4)$  and

$$\delta_1 = -Q_0(\eta_1), \quad \delta_2 = -Q_0(\eta_2), \tag{6}$$

$$\xi = \lambda^4 + 4\lambda^2, \quad \eta = (5 + 3\sqrt{3})^{\frac{1}{2}}. \tag{7}$$

In the absence of multiple roots, the simple roots of  $Q_d(x)$ ,  $\alpha_i, i \in \{1, 2, 3, 4\}$ , can be classified according to the values of the above parameters as shown in table 1.

Our first task will be to explore the set of solutions of (5). For any  $\lambda \geq 0, d > 0$ , we have that  $\alpha_1 < -\lambda < \alpha_2$ , and also that  $Q_d(x) \geq 0$  as long as  $\alpha_1 \leq x \leq \alpha_2$  or  $\alpha_3 \leq x \leq \alpha_4$ . Using standard arguments and formulae I.3.145 and I.3.147 of [4] we can solve (5). For those cases

in which the values of  $\lambda$  and  $d$  give rise to four roots,  $\alpha_1 < \alpha_2 < \alpha_3 < \alpha_4$  of  $Q_d(x)$ , we obtain two solutions of (5). The first one is given by

$$\kappa_d^\lambda(s) = \frac{\alpha_2(\alpha_4 - \alpha_1) - \alpha_4(\alpha_2 - \alpha_1) \operatorname{cn}^2(rs, M)}{(\alpha_4 - \alpha_1) - (\alpha_2 - \alpha_1) \operatorname{cn}^2(rs, M)}, \tag{8}$$

where

$$r = \frac{\sqrt{(\alpha_4 - \alpha_2)(\alpha_3 - \alpha_1)}}{4}, \quad M = \sqrt{\frac{(\alpha_4 - \alpha_3)(\alpha_2 - \alpha_1)}{(\alpha_4 - \alpha_2)(\alpha_3 - \alpha_1)}}$$

and  $\operatorname{cn}(rs, M)$  is the Jacobi elliptic cosine. The curvature function  $\kappa_d^\lambda(s)$  oscillates between  $\alpha_1 = \kappa_d^\lambda(0)$  and  $\kappa_d^\lambda\left(\frac{K(M)}{r}\right) = \alpha_2$ ,  $K(M)$  being the complete elliptic integral of the first kind. The second solution  $\tilde{\kappa}_d^\lambda(s)$  is obtained by interchanging  $1 \leftrightarrow 3, 2 \leftrightarrow 4$  in the right term of (8). This time it oscillates between  $\alpha_3 = \tilde{\kappa}_d^\lambda(0)$  and  $\tilde{\kappa}_d^\lambda\left(\frac{K(M)}{r}\right) = \alpha_4$ . If we denote by  $\gamma_d^\lambda(s), \tilde{\gamma}_d^\lambda(s)$  the (unique, up to rigid motions) curves in  $\mathbb{S}^2(1)$  whose curvatures are  $\kappa_d^\lambda(s)$  and  $\tilde{\kappa}_d^\lambda(s)$  respectively, then they are both convex curves (that is, the curvature is a non-negative function) if  $\lambda^2 > 5 + 3\sqrt{3}$  and  $d < \lambda^4 + 4\lambda^2$ . One curve is convex but not the other one, otherwise. Analogously, for those cases in which the values of the parameters  $\lambda$  and  $d$  produce two simple roots  $\alpha_1 < \alpha_2$ , the solution of (5) is given by

$$\begin{aligned} \kappa_d^\lambda(s) = & \frac{(p+q)(q\alpha_2 + p\alpha_1) - 2pq(\alpha_2 - \alpha_1) \operatorname{cn}(rs, M)}{(p+q)^2 - (p-q)^2 \operatorname{cn}^2(rs, M)} + \dots \\ & + \frac{(p-q)(q\alpha_2 - p\alpha_1) \operatorname{cn}^2(rs, M)}{(p+q)^2 - (p-q)^2 \operatorname{cn}^2(rs, M)}, \end{aligned} \tag{9}$$

with

$$p^2 = (\alpha_2 + \alpha_1)^2 + 2\alpha_2^2 - 2\lambda^2 + 4, \quad M = \frac{1}{2} \sqrt{\frac{(\alpha_2 - \alpha_1)^2 - (p-q)^2}{pq}}, \tag{10}$$

$$q^2 = (\alpha_2 + \alpha_1)^2 + 2\alpha_1^2 - 2\lambda^2 + 4, \quad r = \frac{\sqrt{pq}}{2}. \tag{11}$$

Now  $\kappa_d^\lambda(s)$  oscillates between  $\alpha_1 = \kappa_d^\lambda(0)$  and  $\kappa_d^\lambda\left(\frac{2K(M)}{r}\right) = \alpha_2$ .

Secondly, we introduce a coordinate system adapted to the problem. In order to ease the notation for given  $\lambda \geq 0$  and  $d > 0$ , the corresponding periodic solution of (5),  $\kappa_d^\lambda(s)$ , will be denoted simply by  $\kappa(s)$ . Let  $\rho$  be its period. Take  $\gamma(s)$  the curve in  $\mathbb{S}^2(1)$  associated with  $\kappa(s)$  and represent its Frenet frame by  $\{T(s), N(s)\}$ . Then, the vector field along  $\gamma(s)$  defined by

$$\mathcal{J} = (\kappa^2 - \lambda^2)T + 2\kappa_s N, \tag{12}$$

can be extended to a Killing field on  $\mathbb{S}^2(1)$  which we also denote by  $\mathcal{J}(s)$  [2, 7]. Choose geographic coordinates,  $x(\theta, \phi) = (\cos \theta \sin \phi, \sin \theta \sin \phi, \cos \phi)$ , so that the equator gives the only integral geodesic of  $\mathcal{J}(s)$

$$x_\theta = b\mathcal{J}. \tag{13}$$

The advantage of this coordinate system lies in which it will allow us to express the closedness condition for critical curves in a simple manner (it will be useful also for numerical computations). Indeed, if we assume that  $\kappa(s_0)$  is a minimum of the curvature of  $\gamma(s)$  and we denote by  $\Sigma$  the integral curve of  $\mathcal{J}(s)$  through  $\gamma(s_0)$ , then both curves are tangent at  $\gamma(s_0)$  by (12). Hence,  $|x_\theta|^2 = \frac{1}{1+\kappa_\Sigma^2}$  at  $\gamma(s_0)$ , where  $\kappa_\Sigma$  denotes the geodesic curvature of  $\Sigma$  and, therefore,  $\kappa_\Sigma(s_0) = \frac{-2}{\kappa(s_0) - \lambda}$ . Combining this with (5) we obtain  $b^2d = 1$ .

Now,  $T(s) = \theta'(s)x_\theta + \phi'(s)x_\phi$  and then  $\theta'(s) = \frac{\langle T, x_\theta \rangle}{\sin^2 \phi}$ . Hence if we make use of (5), (12) and (13) we obtain

$$\theta_s(s) = \frac{\kappa^2 - \lambda^2}{b(d - 4(\kappa + \lambda)^2)}, \quad b^2(d - 4(\kappa + \lambda)^2) = \sin^2 \phi. \tag{14}$$

Thus, by using the above notation, we have the following closedness condition [2].

**Proposition 1.** *Let  $\gamma(s)$  be a curve in  $\mathbb{S}^2(1)$  corresponding to a periodic solution of (5)  $\kappa(s)$  with period  $\rho$ . Then  $\gamma(s)$  is a closed  $\lambda$ -elastic curve, if and only if, its progression angle in one period of its curvature,*

$$\Lambda^\lambda(d) = \sqrt{d} \int_0^\rho \frac{(\kappa^2 - \lambda^2)}{d - 4(\kappa + \lambda)^2} ds, \tag{15}$$

is a rational multiple of  $\pi$ .

Our final task in this section will be to show that, for any real number  $\lambda \geq 0$ , the above closedness condition is fulfilled by an infinite family of  $\lambda$ -elastic curves. Thus, we want to investigate the range of variation of  $\Lambda^\lambda(d)$  as  $d$  moves in  $(0, +\infty)$ .

Fix  $\lambda \geq 0$  and assume  $d > 0$ . Then the polynomial  $Q_d(x)$  may have either two real roots  $\alpha_1 \leq \alpha_2$ , or four real roots  $\alpha_1 \leq \alpha_2 \leq \alpha_3 \leq \alpha_4$ . If  $Q_d(x)$  has two simple roots, we consider the solution of (5) given by (9). If it has four simple roots, we select the solution  $\kappa(s)$  which moves between  $\alpha_1$  and  $\alpha_2$  given by (8). Then, we define  $\Lambda^\lambda : (0, \infty) \rightarrow \mathbb{R}$  by (15). Using (5) this function turns out to be

$$\Lambda^\lambda(d) = \sqrt{d} \int_{\alpha_1}^{\alpha_2} \frac{(\kappa^2 - \lambda^2)}{(d/4 - (\kappa + \lambda)^2)\sqrt{Q_d(\kappa)}} d\kappa. \tag{16}$$

As always,  $\gamma(s)$  denotes the curve of  $\mathbb{S}^2(1)$  which is determined by  $\kappa(s)$ . We see that  $\Lambda^\lambda(d)$  moves continuously as  $d$  moves in  $(0, +\infty)$  with two exceptions: (a) those cases in which  $d$  gives rise to multiple roots of  $Q_d(\kappa)$ ; (b) if  $d = 16\lambda^2$ . Multiple roots of  $Q_d(x)$  affect the integrability of (16). On the other hand, if we have  $d = 16\lambda^2$  and the values of  $\lambda$  and  $d$  give rise to two roots of  $Q_d(x)$ , then we get that  $\alpha_2 = \lambda$  is a root of  $Q_d(\kappa)$ . Hence  $\kappa\left(\frac{K(M)}{r}\right) = \alpha_2 = \lambda$  and  $\kappa_s\left(\frac{K(M)}{r}\right) = 0$ . Thus,  $\mathcal{J}(s)$  as given by (12), vanishes at  $s_2 = \frac{K(M)}{r}$ , so that the corresponding curve  $\gamma(s)$  passes at  $s_2$  through a pole of  $\mathbb{S}^2(1)$  for the selected parametrization (13). Therefore  $d = 16\lambda^2$  causes a gap of length  $2\pi$  in  $\Lambda^\lambda(d)$ . If  $d = 16\lambda^2$  and the values of  $\lambda, d$  give rise to four roots of  $Q_d(x)$ , then we would have that  $\alpha_4 = \lambda$  is a root of  $Q_d(\kappa)$  and a similar argument is valid in this case. Now, for a fixed  $\lambda$ , we wish to know how  $\Lambda^\lambda(d)$  behaves as  $d$  approaches to the extremes of its intervals of continuity. This analysis has been made in appendix B.

We set

$$\Lambda_1 = -4\lambda \frac{K(M)}{r} + 8\lambda^2 \int_\zeta^\lambda \frac{d\kappa}{(\kappa + 3\lambda)\sqrt{(\lambda - \kappa)(\kappa - \zeta)((\kappa - u)^2 + v^2)}}, \tag{17}$$

where  $M$  and  $r$  are given in (10) and (11),  $K(M)$  denotes the complete elliptic integral of the first kind, and  $\zeta$  is the only negative root of  $\beta^3 + \lambda\beta^2 + \beta(\lambda^2 - 4) - \lambda(\lambda^2 - 12) = 0$ .

In view of proposition 1, lemma 5 of appendix B and the fundamental theorem for curves in real space forms (which guarantees that a curve in  $\mathbb{S}^2(1)$  is totally determined by its curvature up to rigid motions), we can obtain a multitude of examples of closed  $\lambda$ -elastic curves in  $\mathbb{S}^2(1)$  as follows.

**Theorem 2.** *Fix a real number  $\lambda \geq 0$  and let  $\mathcal{F}^\lambda(\gamma) = \int_\gamma (\kappa + \lambda)^2 ds$  be the elastic energy functional acting on the space of closed immersed curves  $\Omega$  of  $\mathbb{S}^2(1)$ . Then, there exist infinitely*

many values of  $d > 0$  for which the corresponding  $\lambda$ -elastic curves (which are completely determined by either (8) or (9)) satisfy the closedness condition given in proposition 1. Therefore, there exist infinitely many closed critical points of  $\mathcal{F}^\lambda(\gamma)$  in  $\mathbb{S}^2(1)$ .

More concretely, looking at table 4 in appendix B more carefully and playing conservative, we can construct a two-parameter family of  $\lambda$ -elastic curves

**Corollary 3.** *Let  $\lambda$  be a non-negative real number and take  $\Lambda_1$  as defined in (17).*

- (i) *If  $0 \leq \lambda < 2\sqrt{2}$ , then for every pair of integer numbers  $m, n \in \mathbb{Z}$  satisfying  $|\frac{\Lambda_1}{2\pi} - \frac{m}{n}| < \frac{1}{2}$ , there exists a closed  $\lambda$ -elastic curve  $\gamma_{mn}(s)$  in  $\mathbb{S}^2(1)$ .*
- (ii) *If  $\lambda \geq 2\sqrt{2}$ , then for every pair of integer numbers  $m, n \in \mathbb{Z}$  satisfying  $\frac{m}{n} < 0$ , there exists a closed  $\lambda$ -elastic curve  $\gamma_{mn}(s)$  in  $\mathbb{S}^2(1)$ .*

*In any of the above cases,  $\gamma_{mn}(s)$  closes up after  $n$  periods of its curvature and  $m$  trips around the equator.*

Above bounds for  $m, n$  in corollary 3 are conservative. This means that there are closed critical points of  $\mathcal{F}^\lambda(\gamma)$  which do not satisfy the above conditions. Also if  $\lambda = 0$ , then  $\Lambda^0(d)$  moves continuously and monotonically in  $(0, 2\pi)$  what implies the uniqueness of the critical points for given values of  $m$  and  $n$ , [7]. From the discussion in lemma 5, we see that if  $\lambda > 0$  then  $\Lambda^\lambda(d)$  is not continuous in  $(0, \infty)$ . Again, from lemmas 5 and 6 we have that uniqueness of solutions does not hold if  $\lambda \geq 2\sqrt{2}$  because  $\Lambda^\lambda(d)$  is not monotonic (see also figure 4(c)). If  $0 < \lambda < 2\sqrt{2}$ , monotonicity is still undetermined, but figure 4(b) suggests that  $\Lambda^\lambda(d)$  is not going to be monotonic either.

Moreover, the choice  $\lambda = 0$  can be seen as a limiting case of that considered in the proof of lemma 5. If  $\lambda = 0$ , then  $\Lambda_1 = \pi$  and we see that for every pair of integer numbers  $m, n \in \mathbb{Z}$  satisfying  $|\frac{m}{n}| < 1$ , there exists a closed classical elastic curve  $\gamma_{mn}(s)$  in  $\mathbb{S}^2(1)$ , [7].

Having in mind a possible classification of the critical points, a better understanding  $\Lambda^\lambda(d)$  would be desirable. Furthermore, establishing the intervals of monotonicity of  $\Lambda^\lambda(d)$  would give us information about uniqueness of the critical curves. Thus, an explicit determination of  $\Lambda^\lambda(d)$  should be helpful for these purposes. This has been done for  $\lambda = 0$  in [7], where using an explicit expression of  $\Lambda^0(d)$  and formula (9) with  $\lambda = 0$ , the authors were able to prove after long computations that the space of classical elastic curves in  $\mathbb{S}^2(1)$  can be indexed one-to-one by pairs of integers  $0 < m < n$ . They also showed that the only stable elastic curves are geodesics. But even if one can determine explicitly  $\Lambda^\lambda(d)$  in general, an extension of the previous procedure for an arbitrary  $\lambda$  can be a very complicated task. To illustrate this point one may want to consult [2], where a special situation included in the case  $\lambda > 2\sqrt{2}$  was considered and we were able to compute  $\Lambda^\lambda(d)$  explicitly. Finally, the next proposition gives us examples of particular interest in what follows, as we shall see later.

**Proposition 4.** *For any  $\lambda \geq 2\sqrt{2}$  there exists a closed 'figure eight'  $\lambda$ -elastic curve in  $\mathbb{S}^2(1)$ .*

**Proof.** On the one hand, we know from lemma 6 of appendix B that  $\Lambda^\lambda(d)$  takes positive values for  $d \gg 0$ . On the other hand, if we take  $\mu$  as in (19), then we see from lemma 5 of appendix B that  $\lim_{d \rightarrow 16\lambda^2+} \Lambda^\lambda(d) = \Lambda_1 + \pi < 0$  if  $8 < \lambda^2 < \mu^2$ , and  $\lim_{d \rightarrow \delta_2+} \Lambda^\lambda(d) = -\infty$ , if  $\mu^2 < \lambda^2$ . Hence, since  $\Lambda^\lambda(d)$  is continuous in  $(16\lambda^2, \infty)$  (respectively, in  $(\delta_2, \infty)$ ) when  $8 < \lambda^2 < \mu^2$  (respectively, when  $\mu^2 < \lambda^2$ ) there exists a certain value of  $d$ ,  $d > 16\lambda^2$  (respectively,  $d > \delta_2$ ) such that  $\Lambda^\lambda(d) = 0$ . Thus, the corresponding curve closes up in one period of the curvature and zero trips around the equator. Now, by making a shape analysis



**Table 2.** Data relative to the curves of figure 3 as  $d$  does not belong to  $(\delta_1, \delta_2)$ .

Curve	$d$	$n$	$n \frac{\Lambda^\lambda(d)}{2\pi}$	$\alpha_1$	$\alpha_2$
1	2127.126 976	15	1	-7.840 702 7270	7.483 051 7274
2	1057.300 042	21	1	-6.927 107 0253	6.402 294 8105
3	631.279 089	1	0	-6.377 402 0659	5.661 988 4651
4	394.721 729	6	-1	-5.956 383 1887	4.958 383 3200
$\delta_2 = 329.254 833 995 939 04 \dots$					
$\delta_1 = 238.745 166 004 060 958 \dots$					
7	225.889 432 00	11	-1	-5.541 655 8645	-1.382 571 6688
8	103.237 699 72	23	-1	-5.091 494 7550	-2.507 537 3881

**Table 3.** Data relative to the curves of figure 3 as  $d$  moves in  $(\delta_1, \delta_2)$ .

Curve	$d$	$n$	$n \frac{\Lambda^\lambda(d)}{2\pi}$	$n \frac{\tilde{\Lambda}^\lambda(d)}{2\pi}$	$\alpha_1$	$\alpha_2$	$\alpha_3$	$\alpha_4$
5	320.956 5512	4	-1	-1	-5.792 487	0.030 717	1.171 036	4.590 732
6	271.178 6235	8	-1	-1	-5.667 985	-0.874 617	2.347 681	4.194 922
$\delta_1 = 238.745 166 004 060 958 \dots$								

similar to that of subsection 3.1, we see that such a critical point is a ‘figure eight’ curve. This concludes the proof. □

### 3. Numerical approach

Our purpose in this section is to address some of the questions outlined in the previous discussion from a numerical point of view. This will include estimation of  $\Lambda_1$ , evaluation of the monotonicity intervals for  $\Lambda^\lambda(d)$  and graphical determination of shape and energy of closed  $\lambda$ -elastic curves.

We use the notation convention introduced just before proposition 1. For a fixed  $\lambda \geq 0$  and any  $d > 0$ , we denote by  $\kappa(s)$  the periodic solution of (5) obtained from  $d$ . Assume that its period is  $\rho$ . Let  $\gamma(s)$  be the critical curve of  $\mathcal{F}^\lambda$  determined by having as the curvature function  $\kappa(s)$ . Moreover,  $\Lambda^\lambda(d)$  as given in (15), and  $\mathcal{E}^\lambda(d)$  which we define by

$$\mathcal{E}^\lambda(d) = \int_0^\rho (\kappa + \lambda)^2 ds, \tag{18}$$

will represent the angular variation and the energy of the critical curve  $\gamma(s)$  in one period of its curvature, respectively. Note that in defining  $\mathcal{E}^\lambda(d)$  we are using the same convention as we did in the definition of  $\mathcal{F}^\lambda$ : if  $Q_d(x)$  has four simple roots, we consider the solution  $\kappa(s)$  which moves between  $\alpha_1$  and  $\alpha_2$  given by (8).

#### 3.1. Shape of closed critical points

Here we obtain some qualitative information about the closed critical points  $\gamma(s)$  which is complemented numerically in tables 2, 3 and figure 3. We just consider the case  $\lambda > \mu$ , where we set

$$\mu = \sqrt{\frac{11}{2} + \frac{5\sqrt{5}}{2}}. \tag{19}$$

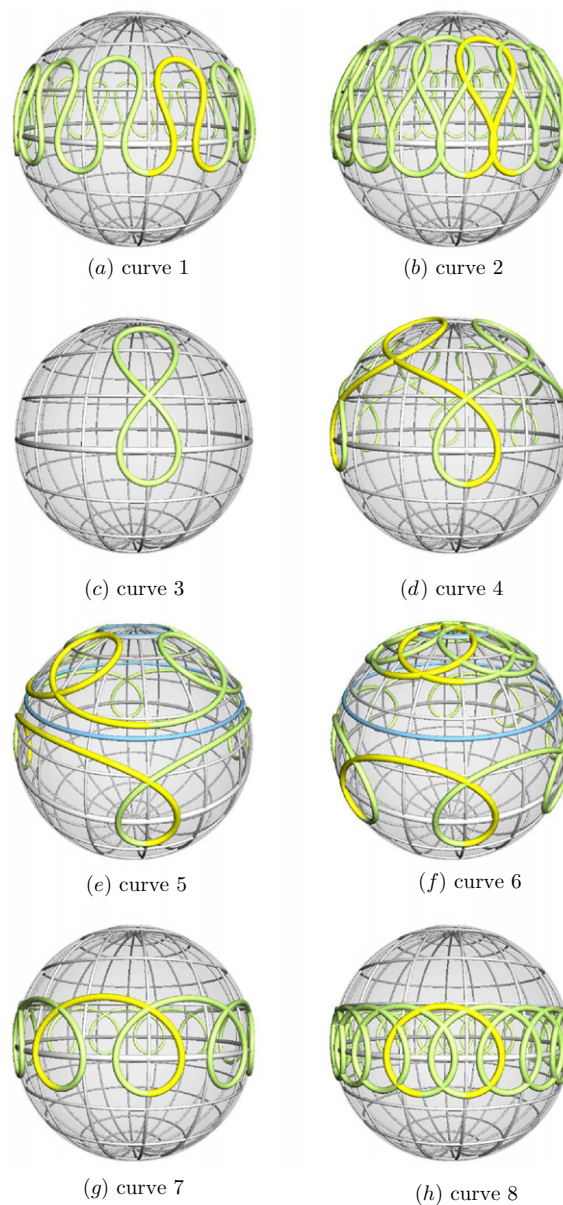


**Figure 3.** Curves corresponding to data in tables 2 and 3.

Other cases can be analysed similarly. Closed critical curves correspond to the values of  $d$  which satisfy the condition (15) as  $d$  moves in  $(0, \delta_2)$ ,  $(\delta_2, \infty)$ . A rough description of critical curves shapes can be given using (4), (5) and (12). From these equations, we see that if  $\gamma(s)$  were a closed  $\lambda$ -elastica in  $\mathbb{S}^2(1)$ , then  $\kappa_{ss}(\bar{s}) = 0$  at a point  $\bar{s}$  would imply that  $\kappa_s(\bar{s}) \neq 0$ , unless  $d = 0, \delta_1$  or  $\delta_2$ . We choose  $d \neq 0, \delta_1, \delta_2$ . Now figure 1 shows the two possible shapes of  $Q_d(x)$ . As we know,  $Q_d(x)$  may have up to four simple roots  $\alpha_i = \kappa(s_i)$ ,  $\alpha_i < \alpha_j, i < j$ ,  $\kappa_s(s_i) = 0, i, j \in \{1, 2, 3, 4\}$ . Using this information in (4), (5), (12) and considering the

coordinate system described in (13), we see that

$$\frac{d|\mathcal{J}|^2}{ds}(s_i) = 0, \quad \frac{d^2|\mathcal{J}|^2}{ds^2}(s_i) = -8[(\kappa + \lambda)\kappa_{ss}](s_i). \quad (20)$$

Start with a large enough value of  $d$ . If  $d$  is greater than  $\delta_2$  and satisfies the closedness condition given by proposition 1, then  $Q_d(x)$  has two roots  $\alpha_i = \kappa(s_i)$ ,  $i \in \{1, 2\}$ , verifying  $\alpha_1 < -\lambda < 0 < \lambda < \alpha_2$ , and the curvature of the closed critical curve moves continuously between its minimum  $\alpha_1 = \kappa(s_1)$  and its maximum  $\alpha_2 = \kappa(s_2)$ . Hence  $\kappa_{ss}(s_1) > 0$ ,  $\kappa_{ss}(s_2) < 0$  and using (20) we have  $\frac{d^2|\mathcal{J}|^2}{ds^2}(s_i) > 0$ ,  $i \in \{1, 2\}$ .

Therefore,  $|\mathcal{J}|^2$  reaches local minima at  $s_i$ ,  $i \in \{1, 2\}$ . Thus  $\gamma(s_i)$ ,  $i \in \{1, 2\}$ , are locally the farthest points to the equator on  $\gamma(s)$ . The closer  $d$  is to  $\delta_2$  the more periods of the curvature and/or trips around the equator the curve  $\gamma(s)$  will need to close up. These curves are embedded until  $d$  reaches the value for what  $\Lambda_{\alpha_1}^\lambda(d)$ , as defined in (B.9), vanishes. At that moment, they start to have multiple points. See figures 3(a)–(d).

If  $\delta_1 < d < \delta_2$ , then for each value of  $d$  satisfying (15),  $Q_d(x)$  has four roots  $\alpha_i = \kappa(s_i)$ ,  $i \in \{1, 2, 3, 4\}$ , verifying  $\alpha_1 < -\lambda < \alpha_2 < \alpha_3 < \lambda < \alpha_4$  and  $0 < \alpha_3$ . Then, two different closed critical curves  $\gamma(s)$  and  $\tilde{\gamma}(s)$  will appear and their respective curvatures  $\kappa(s)$ ,  $\tilde{\kappa}(s)$  satisfy  $\alpha_1 \leq \kappa(s) \leq \alpha_2$  and  $0 < \alpha_3 \leq \tilde{\kappa}(s) \leq \alpha_4$ . That is,  $\tilde{\gamma}(s)$  is always convex. Moreover, if  $\lambda$  verifies  $\lambda^2 < 5 + 3\sqrt{3}$ , then  $\gamma(s)$  is not convex for any value of  $d$ . If  $\lambda^2 > 5 + 3\sqrt{3}$ , then  $\gamma(s)$  is not convex either unless  $d < \xi = \lambda^4 + 4\lambda^2$ , in which case  $0 < \alpha_0$  and it turns out to be convex.

Assume that  $\kappa(s)$  reaches its minimum at  $s_1$ ,  $\alpha_1 = \kappa(s_1)$  and its maximum at  $s_2$ ,  $\alpha_2 = \kappa(s_2)$ . Hence, as in the previous case,  $\kappa_{ss}(s_1) > 0$ ,  $\kappa_{ss}(s_2) < 0$  and using (20) we have  $\frac{d^2|\mathcal{J}|^2}{ds^2}(s_i) > 0$ ,  $i \in \{1, 2\}$ . Therefore,  $|\mathcal{J}|^2$  reaches local minima at  $s_i$ ,  $i \in \{1, 2\}$  and  $\gamma(s_i)$ ,  $i \in \{1, 2\}$  are locally the farthest points to the equator on  $\gamma(s)$ . Observe that there are points where  $-\lambda = \kappa(s_0)$ . At those points  $\gamma(s)$  crosses the equator. See the lower curves in figures 3(e) and (f).

Now, assume that  $\tilde{\kappa}(s)$  reaches its minimum at  $s_3$ ,  $\alpha_3 = \tilde{\kappa}(s_3)$ , and its maximum at  $s_4$ ,  $\alpha_4 = \tilde{\kappa}(s_4)$ . Then  $\tilde{\kappa}_{ss}(s_3) > 0$  and  $\tilde{\kappa}_{ss}(s_4) < 0$  and using again (20) we have  $\frac{d^2|\mathcal{J}|^2}{ds^2}(s_3) < 0$ , and  $\frac{d^2|\mathcal{J}|^2}{ds^2}(s_4) > 0$ . Therefore,  $|\mathcal{J}|^2$  reaches local maximum at  $s_3 > 0$  and local minimum at  $s_4$ . Hence,  $\tilde{\gamma}(s_3)$  is locally the closest point of  $\tilde{\gamma}(s)$  to the equator and  $\tilde{\gamma}(s_4)$  is locally the farthest one. This time there are no points where  $-\lambda = \kappa(s_0)$  and  $\tilde{\gamma}_d(s)$  does not cross the equator. See the upper curves in figures 3(e) and (f).

As  $d$  continues descending, the progression angles  $\Lambda^\lambda(d)$  of the coupled curves ( $\gamma(s)$ ,  $\tilde{\gamma}(s)$ ) are the same and they need the same number of periods of their curvature to close up. This situation is maintained until  $d$  reaches the curve  $d = 16\lambda^2$ . At that point  $\tilde{\gamma}(s)$  crosses the north pole of the sphere and then its progression angle increases by  $2\pi$  with respect to that of  $\gamma(s)$ .

Finally, if  $0 < d < \delta_1$ , then we have just one closed critical curve for any  $d$  satisfying the closedness condition and  $Q_d(x)$  has two real roots  $\alpha_i = \kappa(s_i)$ ,  $i \in \{1, 2\}$  verifying  $\alpha_1 < -\lambda < \alpha_2 < 0$ . By making a similar discussion, we obtain a situation analogous to the previous one, see figures 3(g) and (h).

If  $\lambda = 4$ , the above discussion is numerically showed in tables 2, 3 and graphically described in figure 3.

### 3.2. Monotonicity intervals for $\Lambda^\lambda(d)$

We know that if  $\lambda = 0$ , then  $\Lambda^\lambda(d)$ , the angular variation of  $\gamma(s)$  in one period of its curvature  $\kappa(s)$ , moves continuously in  $(0, 2\pi)$  as  $d$  moves in  $(0, \infty)$  [7]. As we showed previously,

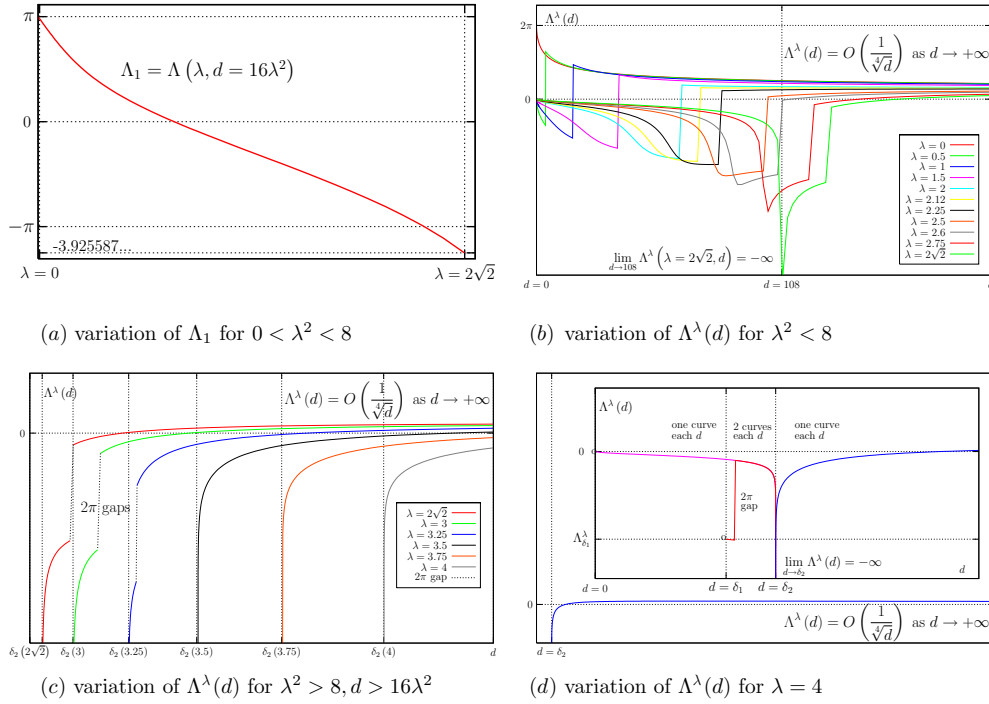


Figure 4. Angular variations  $\Lambda^\lambda(d)$  for different values of  $\lambda$ .

Table 4. Asymptotic behaviour of  $\Lambda^\lambda(d)$ .

$\lambda$	Intervals of continuity of $\Lambda^\lambda(d)$	Variation of $\Lambda^\lambda(d)$
$\lambda = 0$	$(0, \infty)$	$\lim_{d \rightarrow 0} \Lambda^\lambda(d) = 2\pi, \lim_{d \rightarrow \infty} \Lambda^\lambda(d) = 0$
$\lambda \in (0, 2\sqrt{2})$	$(0, 16\lambda^2)$	$\lim_{d \rightarrow 0} \Lambda^\lambda(d) = 0, \lim_{d \rightarrow 16\lambda^2-} \Lambda^\lambda(d) = \Lambda_1 - \pi$
	$(16\lambda^2, \infty)$	$\lim_{d \rightarrow 16\lambda^2+} \Lambda^\lambda(d) = \Lambda_1 + \pi, \lim_{d \rightarrow \infty} \Lambda^\lambda(d) = 0$
	$(0, 108)$	$\lim_{d \rightarrow 0} \Lambda^\lambda(d) = 0, \lim_{d \rightarrow 108-} \Lambda^\lambda(d) = -\infty$
$\lambda = 2\sqrt{2}$	$(108, 128)$	$\lim_{d \rightarrow 108+} \Lambda^\lambda(d) = -\infty, \lim_{d \rightarrow 128-} \Lambda^\lambda(d) = \Lambda_1 - \pi$
	$(128, \infty)$	$\lim_{d \rightarrow 128+} \Lambda^\lambda(d) = \Lambda_1 + \pi, \lim_{d \rightarrow \infty} \Lambda^\lambda(d) = 0$
	$(0, \delta_2)$	$\lim_{d \rightarrow 0} \Lambda^\lambda(d) = 0, \lim_{d \rightarrow \delta_2-} \Lambda^\lambda(d) = -\infty$
$\lambda \in (2\sqrt{2}, \mu)$	$(\delta_2, 16\lambda^2)$	$\lim_{d \rightarrow \delta_2+} \Lambda^\lambda(d) = -\infty, \lim_{d \rightarrow 16\lambda^2-} \Lambda^\lambda(d) = \Lambda_1 - \pi$
	$(16\lambda^2, \infty)$	$\lim_{d \rightarrow 16\lambda^2+} \Lambda^\lambda(d) = \Lambda_1 + \pi, \lim_{d \rightarrow \infty} \Lambda^\lambda(d) = 0$
	$\lambda > \mu$	$(0, \delta_2)$
$(\delta_2, \infty)$		$\lim_{d \rightarrow \delta_2+} \Lambda^\lambda(d) = -\infty, \lim_{d \rightarrow \infty} \Lambda^\lambda(d) = 0$

this is no longer true for the other values of  $\lambda$ . In accordance with the five cases described in table 4, we give a graphical estimation of  $\Lambda^\lambda(d)$  in figure 4.

As we obtained in corollary 3, if  $\lambda \geq 2\sqrt{2}$  then for any choice of  $n \in \mathbb{Z} - \{0\}$  and any choice of a natural number  $m$  we can find a closed curve  $\gamma_{mn}$  in  $\mathbb{S}^2(1)$ , which is a critical point of  $\mathcal{F}^\lambda(\gamma)$  and that closes up in  $n$  periods of its curvature and after  $m$  trips around the equator. This statement is no longer true when  $0 \leq \lambda < \sqrt{2}$ . For instance, if  $\lambda = 0$  we must have  $0 < m < n$  in order to have a closed classical elastica  $\gamma_{mn}$  having the above properties. Moreover monotonicity of  $\Lambda^0(d)$  implies the uniqueness of critical curves  $\gamma_{mn}$  when they

exist, [7]. If  $0 < \lambda < 2\sqrt{2}$  figure 4(b) suggests that, for a certain  $\nu > 0$ , we are going to have uniqueness in the above sense if  $0 < \lambda < \nu$ , but that we lose uniqueness if  $\lambda$  goes beyond such a  $\nu$ . We also know from our discussion in the proof of lemma 5 in appendix B, that in this case  $\Lambda^\lambda(d)$  has a gap of length  $2\pi$  when  $d = 16\lambda^2$  (which is shown in figure 4(b)). The centre of this gap is measured by the number  $\Lambda_1$  defined in (17). A graphical estimation of  $\Lambda_1$  for  $0 < \lambda < 2\sqrt{2}$  is given in figure 4(a). It shows that  $\Lambda_1$  decreases from  $\pi$  to a value close to  $-3.925\,587$  as  $\lambda$  goes from 0 to  $2\sqrt{2}$ .

However, from our discussion following corollary 3, we see that uniqueness of critical points for a given  $d$  does not hold when  $\lambda \geq 2\sqrt{2}$ . The picture of figure 4(c) shows indeed, that for values of  $m, n$  close to 0 we are going to have two closed critical curves  $\gamma_{mn}, \tilde{\gamma}_{mn}$  which close up in  $n$  periods of its curvature and after  $m$  trips around the equator. But looking at figure 4(c) again, we see that if  $\lambda \geq 2\sqrt{2}$ , apparently the branch of  $\Lambda^\lambda(d)$  corresponding to  $d \in (\delta_2, \infty)$  always crosses the  $d$ -axis, reaches a maximum and decreases asymptotically to 0 after that. This fact is confirmed in lemmas 5 and 6. It means that we still have another closed critical curve  $\bar{\gamma}_{mn}$  of  $\mathcal{F}^\lambda(\gamma)$  which also close up after the same number of periods and trips around the equator, but rotating in the reverse sense as that of  $\gamma_{mn}$ . The closed ‘figure eight’  $\lambda$ -elastic curve that appears in proposition 4 corresponds to the value of  $d$  which makes  $\Lambda^\lambda(d) = 0$ .

### 3.3. Energy of closed $\lambda$ -elastic curves

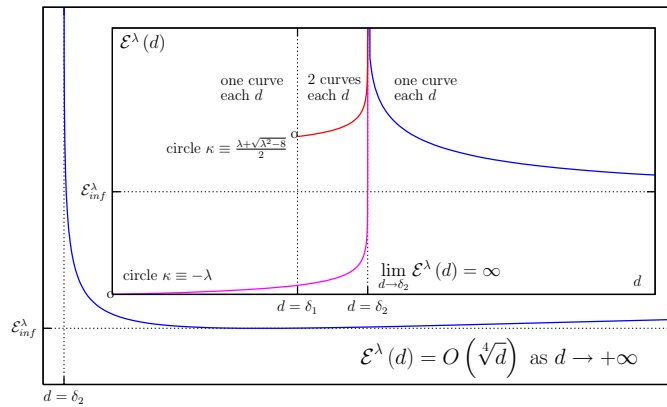
Now that we have a reasonable knowledge of the critical points of  $\mathcal{F}^\lambda(\gamma)$ , we would like to numerically search for its minima. Obviously, circles of curvature  $\kappa = -\lambda$  are global minima. If  $\lambda^2 \leq 8$ , there are no more critical circles. If  $\lambda^2 \geq 8$ , there are two more critical circles,  $C_{\eta_1}, C_{\eta_2}$ , with curvatures  $\eta_1 = \frac{\lambda + \sqrt{\lambda^2 - 8}}{2}$  and  $\eta_2 = \frac{\lambda - \sqrt{\lambda^2 - 8}}{2}$ , respectively. We have computed the second variation formula of  $\mathcal{F}^\lambda(\gamma)$  in [2] and showed that  $C_{\eta_2}$  is always unstable and that the once covered  $C_{\eta_1}$  is stable (multiple  $m$ -covers of this circle  $C_{\eta_1}^m$ , are stable provided  $m$  is not too large, proposition 1.4, [2]).

For any  $\lambda \geq 0, d > 0$ , we have defined  $\mathcal{E}^\lambda(d)$  in (18) as the energy of the critical curve  $\gamma(s)$  in one period  $\rho$  of its curvature  $\kappa(s)$ . By observing figure 5(b), which shows the graphic of  $\mathcal{E}^\lambda(d)$  for a value of  $\lambda$  verifying  $\lambda^2 \leq 8$ , it seems that, in this case, the only minimum of  $\mathcal{E}^\lambda(d)$  is obtained as  $d \rightarrow 0^+$ . It corresponds to the global minimum given by the circle of constant curvature  $\kappa = -\lambda$ . *This circle is the only stable critical point for  $\lambda = 0$ , the classical elastica case [7].* The situation changes drastically if  $\lambda^2 \geq 8$ . To clarify ideas, we take again  $\lambda = 4$ . Then, the energy function on this family of critical curves is represented in figure 5(a). The intervals of continuity of  $\Lambda^\lambda(d)$  when  $\lambda = 4$  are  $(0, \delta_2), (\delta_2, \infty)$ . If  $\delta_1 < d < \delta_2$ , for each value of  $d$  satisfying the closedness condition (proposition 1),  $Q_d(x)$  has four roots  $\alpha_i = \kappa(s_i)$ ,  $i \in \{1, 2, 3, 4\}$ . Thus, two closed critical curves will appear  $\gamma(s)$  and  $\tilde{\gamma}(s)$  with respective curvatures  $\kappa(s)$  and  $\tilde{\kappa}(s)$  verifying  $\alpha_1 \leq \kappa(s) \leq \alpha_2$  and  $0 < \alpha_3 \leq \tilde{\kappa}(s) \leq \alpha_4$ . If  $d$  is not in  $(\delta_1, \delta_2)$ , then for each value of  $d$  satisfying the closedness condition,  $Q_d(x)$  has two roots  $\alpha_i = \kappa(s_i), i \in \{1, 2\}$ , and there is only one closed critical curve  $\gamma(s)$  whose curvature  $\kappa(s)$  verifies  $\alpha_1 \leq \kappa(s) \leq \alpha_2$ . Now, for  $\lambda = 4$ , we denote the energy simply by

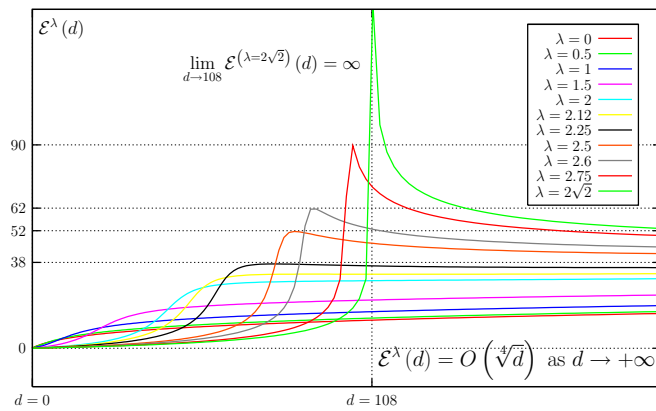
$$\mathcal{E}(d) = \int_0^\rho (\kappa + 4)^2 \quad (21)$$

if  $d \in (0, \delta_2) \cup (\delta_2, \infty)$ , and define

$$\tilde{\mathcal{E}}(d) = \int_0^\rho (\tilde{\kappa} + 4)^2 \quad (22)$$



(a)  $\lambda = 4$

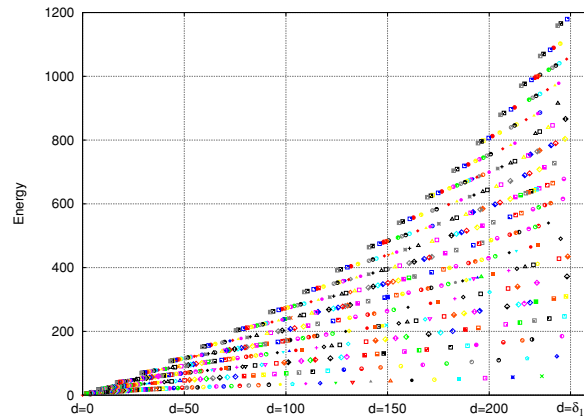


(b)  $\lambda^2 \leq 8$

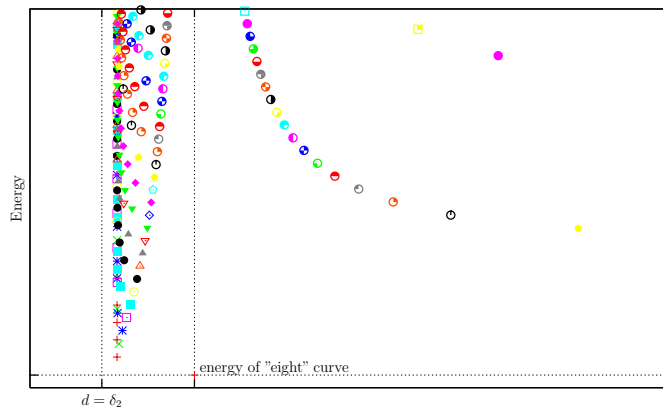
Figure 5. Variation of the  $\mathcal{E}^\lambda(d)$  for different values of  $\lambda$ .

if  $d \in (\delta_1, \delta_2)$ . A numerical evaluation of both functions is given in figure 5(a). The upper graph in the interval  $(\delta_1, \delta_2)$  corresponds to  $\tilde{\mathcal{E}}(d)$ . As we know there are three closed critical curves of constant curvatures  $C_{\eta_0}, C_{\eta_1}$  and  $C_{\eta_2}$ . The minimum value of  $\mathcal{E}(d)$ , as  $d \rightarrow 0^+$  (respectively, of  $\tilde{\mathcal{E}}(d)$  as  $d \rightarrow \delta_1^+$ ) that we see in figure 5(a), corresponds to  $C_{\eta_0}$  (respectively,  $C_{\eta_1}$ ). As it is apparent from the picture, the circle  $C_{\eta_0}$  of curvature  $\eta_0 = -\lambda$  is a (global) minimum for  $\mathcal{E}(d)$ , but the circle of curvature  $\eta_2$  is not. Analogously, the circle of curvature  $\eta_1$  is a (local) minimum for  $\tilde{\mathcal{E}}(d)$ . These facts were formally proved in [2] as previously noted. Moreover, since  $\lim_{d \rightarrow 0^+} \Lambda^\lambda(d) = 0$  if  $\lambda = 4$ , then for any choice of a natural number  $n$  (respectively,  $m$ ) we can find a sequence of closed critical curves of  $\mathcal{F}^\lambda(d)$  which close up in  $n$  periods of their curvatures (respectively, after  $m$  trips around the equator) and whose energy  $\mathcal{E}(d)$  converges to 0. See figures 4(d), 5(a) and observe that 0 is the energy in one period of the circle with curvature  $-\lambda$ .

An important remark comes from figure 5(a). We can prove that  $\lim_{d \rightarrow \delta_2^+} \mathcal{E}(d) = \lim_{d \rightarrow \infty} \mathcal{E}(d) = \infty$  and that  $\mathcal{E}(d)$  reaches a minimum in  $(\delta_2, \infty)$  which is denoted by  $\mathcal{E}_{\text{inf}}$ . Furthermore, we may consider the ‘eight figure’ closed critical point  $\beta(s)$  obtained in proposition 4, which corresponds to the value of  $d_\beta \in (\delta_2, \infty)$  that makes  $\Lambda^4(d_\beta) = 0$  (see figure 3(c)). It closes up in one period of its curvature, its energy in one period is close enough



(a) energy of  $C_{\eta_0}$



(b) energy of  $\beta(s)$

**Figure 6.** Variation of the  $\mathcal{F}^\lambda(d)$  energy for  $\lambda = 4$ .

to  $\mathcal{E}_{\text{inf}}$  and there is a sequence of closed non-convex critical curves whose angular variation in one period approaches to that of  $\beta$ , (see figure 4(d)). Moreover, curves in this sequence need more than one period of their curvature to close up. Therefore, these facts suggest that, for  $\lambda = 4$ , there exists a closed critical curve of non-constant curvature  $\beta(s)$  which is also a local minimum for the energy  $\mathcal{F}^\lambda(d)$ .

A numerical confirmation of this is given in figure 6. Figure 6(a) shows the total energy  $\mathcal{F}^\lambda(d)$  (for  $\lambda = 4$ ) achieved on all the closed critical curves that we obtain as  $d \rightarrow 0^+$  (that is, as the critical points ‘approach’ to the circle  $C_{\eta_0}$  of curvature  $-\lambda$ ) and that need at most 200 periods of their curvature to close up. The minimum, of course, is obtained at  $C_{\eta_0}$ . On the other hand, figure 6(b) shows the total energy  $\mathcal{F}^\lambda(d)$  (for  $\lambda = 4$ ) achieved on all the closed non-convex critical curves that we obtain as  $d \rightarrow d_\beta$  (that is, as the critical points ‘approach’ to the ‘eight’ curve  $\beta(s)$ ) and that need at most 200 periods of their curvature to close up. In this case, the minimum is obtained at  $\beta(s)$ . This numerical fact, if it were formally confirmed, would set a neat difference with the classical elastic curve case, since the only stable closed classical elastica are geodesics, [7]. Experimental results suggest that if  $\lambda^2 > 8$ , the situation resembles to that of case  $\lambda = 4$ .

Finally, we want to give some concluding remarks that arise from our last comments. The second variation formula of  $\mathcal{F}^\lambda$ , as given in [1, 2], was derived for normal variations. In such a form, it is useful to study the stability of critical points with simple curvature (as circles). It has been used also to investigate the stability of other critical points, once a normal variation is known which is a strong candidate to be source of instability (see, for instance, theorem 3.1 of [7]). This approach encounters serious computational difficulties if we want to check out (even numerically) the stability of, for example, the ‘eight figure’ whose curvature is given in (9).

On the other hand, it is plausible to expect that a standard version of the second variation formula can be computed and that it will lead to generalized notions of index form, Jacobi fields and conjugate points for  $\lambda$ -elastic curves. Then, one would expect that conditions to be satisfied by minimizers of  $\mathcal{F}^\lambda$  might be established in terms of conjugate points. Hence, one might try to compute (at least numerically) the lowest eigenvalues in order to check out the local minimizing character of the ‘eight figure’.

These considerations fall out of the scope of this paper and may set the path for future investigations.

### Acknowledgments

This research was partially supported by a MEC grant MTM2004-04934-C04-03 and a UPV grant 9/UPV00127.310-15841/2004. We wish to express our sincere thanks to the referees for their valuable comments and detailed suggestions for improving the manuscript.

### Appendix A

Let  $\gamma(t)$  be a  $C^\infty$  curve immersed in the two-dimensional standard unit sphere,  $\gamma : [0, 1] \rightarrow \mathbb{S}^2(1)$ . We denote by  $v(t) = \|\gamma'(t)\|$  and  $\kappa(t)$  its speed and curvature respectively. As usual, we also denote by  $s$  the arclength parameter and by  $\gamma(s), \kappa(s)$  the corresponding reparametrizations. Let  $\{T(s), N(s)\}$  be the Frenet frame along  $\gamma(s)$ , then the Frenet equations are given by

$$\nabla_T T = \kappa N, \quad \nabla_T N = -\kappa T. \quad (\text{A.1})$$

Now, we consider the functional  $\mathcal{F}^\lambda(\gamma) = \int_\gamma (\kappa + \lambda)^2 ds$ , acting on a suitable space  $\Omega$  of immersed curves in  $\mathbb{S}^2(1)$ . For example,  $\Omega$  can be the space of closed curves or it may be formed by curves satisfying appropriate first-order boundary data. Then, in order to derive the first variation formula for  $\mathcal{F}^\lambda$ , we take a variation of  $\gamma : [0, 1] \rightarrow \mathbb{S}^2(1)$  within the specified space of curves,  $\Gamma = \Gamma(t, r) : [0, 1] \times (-\varepsilon, \varepsilon) \rightarrow \mathbb{S}^2(1)$  with  $\Gamma(t, 0) = \gamma(t)$ . Associated with this variation is the variation vector field along the curve  $\gamma(t)$ ,  $W = W(t) = \frac{\partial \Gamma}{\partial r}(t, 0)$ . We also write  $V = V(t, r) = \frac{\partial \Gamma}{\partial t}(t, r)$ ,  $W = W(t, r)$ ,  $v = v(t, r)$ ,  $T = T(t, r)$ ,  $N = N(t, r)$ , etc, with the obvious meanings. We let  $V(s, r), W(s, r)$ , etc, denote the corresponding reparametrizations. The following formulae were obtained in [7]

$$W(v) = \langle \nabla_T W, T \rangle v, \quad (\text{A.2})$$

$$W(\kappa) = \langle \nabla_T^2 W, N \rangle - 2\kappa \langle \nabla_T W, T \rangle + \langle W, N \rangle. \quad (\text{A.3})$$

Using formulae (A.2), (A.3) and integration by parts, one gets

$$\delta \mathcal{F}^\lambda(\gamma)[W] = \int_\gamma \langle \mathcal{E}(\gamma), W \rangle ds + [\mathcal{B}(\gamma, W)]_0^1, \quad (\text{A.4})$$



where  $\mathcal{E}(\gamma)$  and  $\mathcal{B}(\gamma, W)$  represent the Euler–Lagrange and boundary operators respectively. They are given by

$$\mathcal{E}(\gamma) = (2\kappa_{ss} + \kappa^3 + (2 - \lambda^2)\kappa + 2\lambda)N, \quad (\text{A.5})$$

$$\mathcal{B}(\gamma, W) = [2\langle \nabla_T W, (\kappa + \lambda)N \rangle - \langle W, 2\kappa_s N + (\kappa^2 - \lambda^2)T \rangle]_0^1. \quad (\text{A.6})$$

Here the subscript  $s$  denotes differentiation with respect to the arclength. The boundary operator  $\mathcal{B}$  vanishes for curves in  $\Omega$ . Hence, by using a standard argument it follows from (A.4) and (A.5) that critical points of  $\mathcal{F}^\lambda$  are characterized by satisfying

$$2\kappa_{ss} + \kappa^3 + (2 - \lambda^2)\kappa + 2\lambda = 0. \quad (\text{A.7})$$

## Appendix B

We consider the angular progression in one period of the curvature  $\Lambda^\lambda(d)$  defined in (15). We need to know how this function behaves within its intervals of continuity. Let  $\delta_2$ ,  $\Lambda_1$  and  $\mu$  be as defined in (6), (17) and (19) respectively. We have the following:

**Lemma 5.** *Fix a real number  $\lambda \geq 0$ . Then the behaviour of  $\Lambda^\lambda(d)$  at the extremes of its intervals of continuity is shown in table 4.*

**Proof.** For the sake of brevity, we just consider here the case  $\lambda \in (0, 2\sqrt{2})$  in some detail. The remaining cases can be analysed similarly. Now,  $Q_d(x)$  has two simple roots  $\alpha_i, i \in \{1, 2\}$ , verifying  $\alpha_1 < -\lambda < \alpha_2$  for any  $d > 0$ , so we must pay attention only to the discontinuity derived from  $d = 16\lambda^2$ . We write (5) in the form

$$\kappa_s^2 = \frac{1}{4}Q(\kappa) = \frac{1}{4}(\kappa - \alpha_1)(\alpha_2 - \kappa)((\kappa - u)^2 + v^2), \quad (\text{B.1})$$

where we have the following relations

$$0 = 2u + \alpha_1 + \alpha_2, \quad d = \lambda^4 + 4\lambda^2 - \alpha_1\alpha_2(u^2 + v^2), \quad (\text{B.2})$$

$$4 - 2\lambda^2 = u^2 + v^2 + \alpha_1\alpha_2 + 2u(\alpha_1 + \alpha_2), \quad (\text{B.3})$$

$$-8\lambda = (u^2 + v^2)(\alpha_1 + \alpha_2) + 2u\alpha_1\alpha_2. \quad (\text{B.4})$$

Hence

$$u = -\frac{(\alpha_1 + \alpha_2)}{2}, \quad v^2 = \frac{3}{4}(\alpha_1 + \alpha_2)^2 - \alpha_1\alpha_2 - 2\lambda^2 + 4, \quad (\text{B.5})$$

$$d = \lambda^4 + 4\lambda^2 - \alpha_1\alpha_2((\alpha_1 + \alpha_2)^2 - \alpha_1\alpha_2 - 2\lambda^2 + 4). \quad (\text{B.6})$$

Using (B.1) we can write

$$\Lambda^\lambda(d) = \int_{\alpha_1}^{\alpha_2} \Upsilon(\kappa, d) \, d\kappa, \quad (\text{B.7})$$

with

$$\Upsilon(\kappa, d) = \frac{\sqrt{d}(\kappa^2 - \lambda^2)}{\left(\frac{d}{4} - (\kappa + \lambda)^2\right) \sqrt{(\alpha_2 - \kappa)(\kappa - \alpha_1)((\kappa - u)^2 + v^2)}}. \quad (\text{B.8})$$

If we take  $d \rightarrow 0^+$ , then one sees from (9), (10) and (11) that the curvature  $\kappa(s)$  approaches to a constant  $-\lambda$ , and that the period of  $\kappa(s)$ ,  $\rho = 4\frac{K(M)}{r}$ , approaches to  $\frac{2\pi}{\sqrt{\lambda^2+1}}$  ( $M$  goes

to 0 and  $r$  to  $\sqrt{\lambda^2 + 1}$ . Thus the limiting shape of the curves which correspond to the solutions of (5) as  $d$  goes to 0 is a circle of curvature  $\kappa \equiv -\lambda$  and radius  $\frac{1}{\sqrt{\lambda^2 + 1}}$ . Since  $\alpha_1 \leq \kappa(s) \leq \alpha_2 < 0, \alpha_1 < -\lambda < \alpha_2$  and, as a consequence of (B.1),  $\kappa(s)$  has no vertices at the points where  $\kappa(s) = -\lambda$ , we see that the Killing vector field  $\mathcal{J}(s)$  given by (12) does not vanish on  $\gamma(s)$ . Thus the limiting circle does not cross the north pole and then  $\lim_{d \rightarrow 0^+} \Lambda^\lambda(d) = 0$ .

On the other hand, we have that  $\lim_{d \rightarrow +\infty} \alpha_1 = -\infty$  and  $\lim_{d \rightarrow +\infty} \alpha_2 = +\infty$ , thus by using (B.5) and (B.6) we obtain  $\lim_{d \rightarrow +\infty} v = +\infty$  and  $\lim_{d \rightarrow +\infty} \left(\frac{v^2}{\alpha_1 \alpha_2}\right) = -1$ . Hence, from (B.2)–(B.4) one gets  $\lim_{d \rightarrow +\infty} u = \lim_{d \rightarrow +\infty} (\alpha_1 + \alpha_2) = 0$ .

Now, let us write (B.7) in the form  $\Lambda^\lambda(d) = \Lambda_{\alpha_1}^{-\lambda}(d) + \Lambda_{-\lambda}^\lambda(d) + \Lambda_{\alpha_2}^{\alpha_2}(d)$ , where

$$\begin{aligned} \Lambda_{\alpha_1}^{-\lambda}(d) &= \int_{\alpha_1}^{-\lambda} \Upsilon(\kappa, d) \, d\kappa, & \Lambda_{-\lambda}^\lambda(d) &= \int_{-\lambda}^\lambda \Upsilon(\kappa, d) \, d\kappa, \\ \Lambda_{\alpha_2}^{\alpha_2}(d) &= \int_{\lambda}^{\alpha_2} \Upsilon(\kappa, d) \, d\kappa. \end{aligned} \tag{B.9}$$

They can be bounded by

$$|\Lambda_{\alpha_1}^{-\lambda}| \leq \frac{4\sqrt{d}(\alpha_1^2 - \lambda^2)}{(d - 4(\alpha_1 + \lambda)^2)\sqrt{(\lambda + u)^2 + v^2}}, \tag{B.10}$$

$$|\Lambda_{-\lambda}^\lambda| \leq \frac{8\lambda^3\sqrt{d}}{(d - 16\lambda^2)^{\frac{3}{2}}}, \tag{B.11}$$

$$|\Lambda_{\alpha_2}^{\alpha_2}| \leq \frac{4\sqrt{d}(\alpha_2^2 - \lambda^2)}{(d - 4(\alpha_2 + \lambda)^2)\sqrt{(\lambda - u)^2 + v^2}}. \tag{B.12}$$

Then, making use of (B.6) we have  $\lim_{d \rightarrow +\infty} \Lambda_{\alpha_1}^{-\lambda} = \lim_{d \rightarrow +\infty} \Lambda_{-\lambda}^\lambda = \lim_{d \rightarrow +\infty} \Lambda_{\alpha_2}^{\alpha_2} = 0$ , and therefore  $\lim_{d \rightarrow +\infty} \Lambda^\lambda(d) = 0$ .

Furthermore, defining  $\Lambda_1$  as in (17), one can prove similarly that  $\lim_{d \rightarrow 16\lambda^2-} \Lambda^\lambda(d) = \Lambda_1 - \pi$  and  $\lim_{d \rightarrow 16\lambda^2+} \Lambda^\lambda(d) = \Lambda_1 + \pi$  (see figures 4(a) and (b)).

As for the remaining cases, we have that the cases  $\lambda = 0$  (studied in [7]) and  $\lambda = 2\sqrt{2}$  can be obtained as limiting cases of the previous one. If  $2\sqrt{2} < \lambda < \mu$ , then  $Q_d(\kappa)$  has two simple roots  $\alpha_1 < -\lambda < \alpha_2$  for any  $d > 0$  with the exception of  $d = \delta_2$ , where  $\delta_2$  is given in (6). If  $d = \delta_2$ , then  $\alpha_2$  becomes a double root and  $\Lambda^\lambda(d)$  diverges. We also have the discontinuity derived from  $d = 16\lambda^2$ . The intervals of continuity are  $(0, \delta_2), (\delta_2, 16\lambda^2), (16\lambda^2, \infty)$ . If  $\lambda > \mu$ ,  $Q_d(\kappa)$  has again two simple roots  $\alpha_1 < -\lambda < \alpha_2$  for any  $d > 0$ , with the exception again of  $d = \delta_2$ . If  $d = \delta_2$  then  $\alpha_2$  becomes a double root and  $\Lambda^\lambda(d)$  diverges. But now we do not have to worry about the discontinuity derived from  $d = 16\lambda^2$ , because  $\alpha_4 = \lambda$  and  $\alpha_2 < \alpha_4$  for any  $d > 0$ . The intervals of continuity are  $(0, \delta_2), (\delta_2, \infty)$ . In all these cases, the behaviour of  $\Lambda^\lambda(d)$  can be analysed as we did a little bit back with  $\lambda \in (0, 2\sqrt{2})$ . It is shown in table 4 and graphically described in figures 4(b)–(d).  $\square$

Finally, the next lemma gives us some additional information about  $\Lambda^\lambda(d)$  which has been used previously.

**Lemma 6.** *For any given real number  $\lambda \geq 0$ , the angular progression  $\Lambda^\lambda(d)$  takes positive values for  $d$  large enough.*

**Proof.** We use the notation of lemma 5. Fix a number  $\lambda \geq 0$  and take  $d \in (\delta_2, \infty)$  large enough so that the polynomial  $Q_d(\kappa)$  has two simple roots satisfying  $\alpha_1 < -\lambda < \lambda < \alpha_2$ .

Define  $\Upsilon(\kappa, d)$  as in (B.8). Assume first that  $\kappa \in (\alpha_1, -\lambda)$ , then we obtain

$$\Upsilon(\kappa, d) \leq \frac{4\sqrt{d}(\alpha_1^2 - \lambda^2)}{(d - 4(\alpha_1 + \lambda)^2)\sqrt{\kappa - \alpha_1}\sqrt{(\alpha_2 + \lambda)((\lambda + u)^2 + v^2)}}, \quad (\text{B.13})$$

$$\Upsilon(\kappa, d) \geq \frac{4(\kappa^2 - \lambda^2)}{\sqrt{d}\sqrt{(\alpha_2 - \alpha_1)(-\lambda - \alpha_1)((\alpha_1 - u)^2 + v^2)}}. \quad (\text{B.14})$$

One can find similar expressions if  $\kappa \in (\lambda, \alpha_2)$ . Moreover, if  $\kappa \in (-\lambda, \lambda)$ , then

$$\frac{4(\lambda^2 - \kappa^2)}{d} \leq |\Upsilon(\kappa)| \leq \frac{4\lambda^2\sqrt{d}}{(d - 16\lambda^2)\sqrt{d - \delta_2}}, \quad (\text{B.15})$$

for  $\lambda > 2\sqrt{2}$ , and

$$\frac{4(\lambda^2 - \kappa^2)}{d} \leq |\Upsilon(\kappa)| \leq \frac{4\lambda^2\sqrt{d}}{(d - 16\lambda^2)\sqrt{d - 16\lambda^2}}, \quad (\text{B.16})$$

for  $\lambda < 2\sqrt{2}$ . Therefore,  $\Lambda_{\alpha_1}^{-\lambda}$  satisfies

$$\Lambda_{\alpha_1}^{-\lambda} \leq \frac{8\sqrt{d}(\alpha_1^2 - \lambda^2)(\sqrt{\lambda - \alpha_1})}{(d - 4(\alpha_1 + \lambda)^2)\sqrt{(\alpha_2 + \lambda)((\lambda + u)^2 + v^2)}} = O\left(\frac{1}{\sqrt[4]{d}}\right),$$

$$\Lambda_{\alpha_1}^{-\lambda} \geq \frac{4}{\sqrt{d}\sqrt{(\alpha_2 - \alpha_1)(-\lambda - \alpha_1)((\alpha_1 - u)^2 + v^2)}} \left(\frac{2}{3}\lambda^3 - \frac{\alpha_1^3}{3} + \lambda^2\alpha_1\right) = O\left(\frac{1}{\sqrt[4]{d}}\right).$$

Hence  $\Lambda_{\alpha_1}^{-\lambda} = O\left(\frac{1}{\sqrt[4]{d}}\right) > 0$ . Analogously, one can prove that  $\Lambda_{\lambda}^{\alpha_2} = O\left(\frac{1}{\sqrt[4]{d}}\right) > 0$ . Finally, for  $\Lambda_{-\lambda}^{\lambda}$  we have

$$O\left(\frac{1}{d}\right) = \frac{16\lambda^3}{3d} \leq |\Lambda_{-\lambda}^{\lambda}| \leq \frac{8\lambda^3\sqrt{d}}{(d - 16\lambda^2)\sqrt{d - \delta_2}} = O\left(\frac{1}{d}\right),$$

if  $\lambda > 2\sqrt{2}$ , and

$$O\left(\frac{1}{d}\right) = \frac{16\lambda^3}{3d} \leq |\Lambda_{-\lambda}^{\lambda}| \leq \frac{8\lambda^3\sqrt{d}}{(d - 16\lambda^2)\sqrt{d - 16\lambda^2}} = O\left(\frac{1}{d}\right),$$

if  $\lambda < 2\sqrt{2}$ . Thus the angular progression satisfies

$$\begin{aligned} \lim_{d \rightarrow +\infty} \sqrt[4]{d} \cdot \Lambda^{\lambda}(d) &= \lim_{d \rightarrow +\infty} \sqrt[4]{d}(\Lambda_{\alpha_1}^{-\lambda} + \Lambda_{-\lambda}^{\lambda} + \Lambda_{\lambda}^{\alpha_2}) \\ &= \lim_{d \rightarrow +\infty} \sqrt[4]{d}(\Lambda_{\alpha_1}^{-\lambda} + \Lambda_{\lambda}^{\alpha_2}) = C > 0. \end{aligned} \quad (\text{B.17})$$

This concludes the proof.  $\square$

## References

- [1] Arroyo J 2001 Presión calibrada total: estudio variacional y aplicaciones al problema de Willmore–Chen *PhD Thesis* (in Spanish) University of the Basque country, Febrero
- [2] Arroyo J and Garay O J 2001 Hopf vesicles in  $\mathbb{S}^3(1)$ . *Global Diff. Geom. The mathematical legacy of A Gray Contemp. Math.* **288** 258–62
- [3] Arroyo J, Garay O J and Mencia J 2006 Closed elastic circles in  $\mathbb{H}^2(-1)$  in preparation
- [4] Gradshteyn I S and Ryzhik I M 1980 *Table of Integrals, Series and Products* (New York: Academic)
- [5] Kamien R 2002 The geometry of soft materials: a primer *Rev. Mod. Phys.* **74** 953–71
- [6] Landau L D and Lifshitz E M 1986 *Theory of Elasticity (Theoretical Physics vol 7)* 3rd edn (Oxford: Butterworth-Heinemann)
- [7] Langer J and Singer D A 1984 The total squared curvature of closed curves *J. Diff. Geom.* **20** 1–22
- [8] Linner A 1998 Curve straightening and the Palais–Smale condition *Trans. Am. Math. Soc.* **350** 3743–65